UNITED STATES PATENT AND TRADEMARK OFFICE

UNITED STATES DEPARTMENT OF COMMERCE
United States Patent and Trademark Office
Address: COMMISSIONER FOR PATENTS
P.O. Box 1450
Alexandria, Virginia 22313-1450
www.uspto.gov

APR 23 2007

APPLICATION NO.	FILING DATE	FIRST NAMED INVENTOR	ATTORNEY DOCKET NO.	CONFIRMATION NO.
10/718,070	11/20/2003	Hendrik F. Hamann	YOR920030368US1 (8728-643	8659

46069   7590   04/12/2007

F. CHAU & ASSOCIATES, LLC
130 WOODBURY ROAD
WOODBURY, NY 11797

EXAMINER
GEORGE, PATRICIA ANN

ART UNIT	PAPER NUMBER
1765	

SHORTENED STATUTORY PERIOD OF RESPONSE	MAIL DATE	DELIVERY MODE
3 MONTHS	04/12/2007	PAPER

Please find below and/or attached an Office communication concerning this application or proceeding.

If NO period for reply is specified above, the maximum statutory period will apply and will expire 6 MONTHS from the mailing date of this communication.

	Application No.	Applicant(s)
Office Action Summary	10/718,070	HAMANN ET AL.
	Examiner	Art Unit	
	Patricia A. George	1765	

-- The MAILING DATE of this communication appears on the cover sheet with the correspondence address --

Period for Reply

A SHORTENED STATUTORY PERIOD FOR REPLY IS SET TO EXPIRE <u>3</u> MONTH(S) OR THIRTY (30) DAYS, WHICHEVER IS LONGER, FROM THE MAILING DATE OF THIS COMMUNICATION.

- Extensions of time may be available under the provisions of 37 CFR 1.136(a). In no event, however, may a reply be timely filed after SIX (6) MONTHS from the mailing date of this communication.
- If NO period for reply is specified above, the maximum statutory period will apply and will expire SIX (6) MONTHS from the mailing date of this communication.
- Failure to reply within the set or extended period for reply will, by statute, cause the application to become ABANDONED (35 U.S.C. § 133). Any reply received by the Office later than three months after the mailing date of this communication, even if timely filed, may reduce any earned patent term adjustment. See 37 CFR 1.704(b).

Status

1)☒ Responsive to communication(s) filed on <u>02 February 2007</u>.

2a)☒ This action is **FINAL**.   2b)☐ This action is non-final.

3)☐ Since this application is in condition for allowance except for formal matters, prosecution as to the merits is closed in accordance with the practice under *Ex parte Quayle*, 1935 C.D. 11, 453 O.G. 213.

Disposition of Claims

4)☒ Claim(s) *1,2,4,5,7-13,22,23 and 26-29* is/are pending in the application.

    4a) Of the above claim(s) _____ is/are withdrawn from consideration.

5)☐ Claim(s) _____ is/are allowed.

6)☒ Claim(s) *1,2,4,5,7-13,22,23,and 26-29* is/are rejected.

7)☐ Claim(s) _____ is/are objected to.

8)☐ Claim(s) _____ are subject to restriction and/or election requirement.

Application Papers

9)☐ The specification is objected to by the Examiner.

10)☐ The drawing(s) filed on _____ is/are: a)☐ accepted or b)☐ objected to by the Examiner.

    Applicant may not request that any objection to the drawing(s) be held in abeyance. See 37 CFR 1.85(a).

    Replacement drawing sheet(s) including the correction is required if the drawing(s) is objected to. See 37 CFR 1.121(d).

11)☐ The oath or declaration is objected to by the Examiner. Note the attached Office Action or form PTO-152.

Priority under 35 U.S.C. § 119

12)☐ Acknowledgment is made of a claim for foreign priority under 35 U.S.C. § 119(a)-(d) or (f).

    a)☐ All   b)☐ Some * c)☐ None of:

      1.☐ Certified copies of the priority documents have been received.

      2.☐ Certified copies of the priority documents have been received in Application No. _____.

      3.☐ Copies of the certified copies of the priority documents have been received in this National Stage application from the International Bureau (PCT Rule 17.2(a)).

    * See the attached detailed Office action for a list of the certified copies not received.

Attachment(s)

1)☒ Notice of References Cited (PTO-892)

2)☐ Notice of Draftsperson's Patent Drawing Review (PTO-948)

3)☐ Information Disclosure Statement(s) (PTO/SB/08)
    Paper No(s)/Mail Date _____.

4)☐ Interview Summary (PTO-413)
    Paper No(s)/Mail Date. _____.

5)☐ Notice of Informal Patent Application

6)☐ Other: _____.

DETAILED ACTION

Claim Rejections - 35 USC § 103

The following is a quotation of 35 U.S.C. 103(a) which forms the basis for all

obviousness rejections set forth in this Office action:

(a) A patent may not be obtained though the invention is not identically disclosed or described as set forth in section 102 of this title, if the differences between the subject matter sought to be patented and the prior art are such that the subject matter as a whole would have been obvious at the time the invention was made to a person having ordinary skill in the art to which said subject matter pertains. Patentability shall not be negatived by the manner in which the invention was made.

This application currently names joint inventors. In considering patentability of the claims under 35 U.S.C. 103(a), the examiner presumes that the subject matter of the various claims was commonly owned at the time any inventions covered therein were made absent any evidence to the contrary. Applicant is advised of the obligation under 37 CFR 1.56 to point out the inventor and invention dates of each claim that was not commonly owned at the time a later invention was made in order for the examiner to consider the applicability of 35 U.S.C. 103(c) and potential 35 U.S.C. 102(e), (f) or (g) prior art under 35 U.S.C. 103(a).

Claims 1, 2, 4, 5, 7, 11, 12, 13, 22, 23 and 26-29 are rejected under 35 U.S.C.

103(a) as being unpatentable over Chen (6,927,410), in view of Lowrey et al

(6,943,365) (herein referred to as Lowrey) evidenced by Hun Seo et al. (Investigation of

Crystallization Behavior of Sputter-Deposited Nitrogen-Doped Amorphous $Ge_2Sb_2Te_5$

Thin Films; Jpn. J. Appl. Phys. Vol.39 (2000) 745-751; Part 1, No. 2B, 28 February

2000).

Chen teaches: a multi-bit phase changing memory device (ab.), including: layers

of phase change material (ab.) separated by layers of conductive interface (ab.),

produced with varying degrees of resistivity (col.2, l.27).

Chen teach a multi-bit phase change memory cell (claim1) or multi-bit phase

change memory (claim 22), where each of said plurality of phase change material layers

has a different height from one another, please refer to: column 1, lines 35 through

column 2, lines 36, where Chen teaches phase change memory devices, such as multi-

bit memory cells, i.e. multi-bit phase change memory cell (claim 1) and i.e. multi-bit phase change memory (claim 22); and see column 8, lines 28-36, where Chen teaches a plurality of phase change material layer with different thicknesses, i.e. where plurality of phase change material layers has a different height from one another. The term thickness is interpreted as a dimension between two surfaces, as opposed to length or width, i.e. used to describe the height of a semiconductor layer.

Although Chen describes the thickness of the phase change material layers may be different from one another, Chen is silent to the height increasing while surface area decrease, of each of the phase change materials along a direction from the first outer conductor layer to the second outer conductive layer, as in claim 1.

It would have been obvious to one of ordinary skill in the art at the time of invention was made, to select any desired height and surface area, of each of the phase change materials along a direction from the first outer conductor layer to the second outer conductive layer, as in applicants' claimed limitation, when forming the multi-bit phase changing memory device, as Chen, because Chen teaches it is effective to provide phase change material layers of varying thickness that are different from one another. In the absence of unexpected results, one of ordinary skill would form the phase change layers as desires, including applicants' specifically claimed height increasing while surface area decrease, of each of the phase change materials along a direction from the first outer conductor layer to the second outer conductive layer, because the reference does not limit the ordered configuration of phase change materials.

Further, because Chen discloses a plurality of phase change material layers with different thicknesses, see column 8, lines 28-36, one of ordinary skill in the art would recognize that the plurality of phase change material layers with different thicknesses, as in the reference of Chen, would also have different surface areas from one another, because the mathematical equation for surface area is dependent on height (i.e. thickness) as a multiplier, and a variety of heights would calculate a result with a variety of surface areas. Applicants' have not shown anything unexpected when forming the claimed ordered configuration of phase change materials.

Chen does not teach the structure of the first and second conductive layers, disposed on opposite sides of the memory cell, as in claim 1.

Lowrey illustrates the first outer conductive layer (130a) disposed at the right side (i.e. one side) of the memory cell and a second outer conductive layer (130b) disposed at the left side (i.e. a side opposite to the one side) of the memory cell, in figure 1A, and refers to this configuration as the "rapier" design of conductor spacer.

It would have been obvious to one of ordinary skill in the art at the time of invention was made, to include the structure of the first and second conductive layers, disposed on opposite sides of the memory cell, as in Lowrey, when forming the multi-bit phase changing memory device, of Chen, because Lowrey teaches this configuration is an improvement as it reduces the size of the area of contact of the memory material, thereby reducing the total current needed to program the memory device.

As to the limitation wherein each of the plurality of phase change material layers have the same resistivity, Chen teaches phase change memory devices use memory materials that are electrically switched (programmed) between different structured states that exhibit different electrical read-out properties. For example, memory devices are programmed between a generally amorphous state that exhibits a relatively high resistivity, and a generally crystalline state that exhibits a relatively low resistivity. The phase change material is programmed by heating the material, whereby the amplitude and duration of the heating dictates whether the phase change material is left in an amorphous or crystallized state. The high and low resistivities represent programmed bit values of "1" and "0", which can be sensed by then measuring the resistivity of the phase change material, which is written on plurality of phase change material layers have the same resistivity (see background, lines 35-52). Chen further teaches first a high current pulse is passed through the memory device to generate a thermal pulse that amorphousizes *all* of the phase change material layers. Then a crystallizing thermal pulse creates a temperature gradient across the memory material, where the various layers are *asymmetrically* heated (i.e. top layers hotter than bottom layers). Over the duration of the crystallizing thermal pulse, the various layers of phase change materials are sequentially crystallized, top down, one layer at a time, which is also written on plurality of phase change material layers have the same resistivity.

It would have been obvious to one of ordinary skill in the art at the time of invention was made, that the programmed bit vaulues of "1" and "0" represent high and low resistivities, which can be sensed by then measuring the resistivity of the phase

change material; that the step which includes a high current pulse, resets all the phase change material layers, preparing them to be programmed with a thermal pulse; and when the high current pulse resets all the phase change material layers they have the same programming value and the same resistivity.

Further on the same topic, Seo et al. provides evidence that nitrogen doping (i.e. implanting) of the $Ge_2Sb_2Te_5$ phase-change films allows the crystalline process to occur in a primary nucleation step, an improved stability of the amorphous phase. Seo et fails to explicitly teach implanting the $Ge_2Sb_2Te_5$ have an effect on the resistivity of the mater, however it would have been obvious to one of ordinary skill in the art at the time of invention was made, that an improvement to the stability of of the amorphous phase of $Ge_2Sb_2Te_5$ that allows the crystalline process to occur in one primary nucleation step would greatly impact the resistivity of the film because it would allow for a change to the state of the resistance to occur more rapidly and remain fixed in that state until another change is desired, therefor allowing all the phase change material layers to be more responsive to holding the same value of resistivity when programmed as less device failure occurs, clearly an improvement in manufacturing.

As for claim 2, Chen illustrates in figure 6, the ability to set the electrical resistance of each of the plurality of phase change material layers in an increasing manner, sequentially, from layer 1 through later 5, pointing to a direction from the first outer conductive layer to the second outer conductive layer.

As for claim 4, Chen's figures 4A-G illustrate wherein each of the plurality of phase change material layers have a different phase transition temperature, also concealed in column 5, lines 23-26.

As for claim 5, Chen explains a method for operating a phase change memory having a volume of memory material, including a plurality of discrete layers of materials. The method includes applying heat to the volume of material for a predetermined amount of time (col.3, l.28-43), which demonstrates the following limitation claimed: each of the plurality of phase change material layers has the same phase transition temperature.

As for claim 7, in figure 3 (explained in col.4, l. 27-49), Chen illustrates a plurality of conductive layers (fig. 3, 26/24/28), including a plurality of intermediate layers (fig.3, 24), disposed between the first (fig.3, 26) and second (fig. 3, 28) outer conductive layers, each of the intermediate conductive layers (fig.3, 24) having the same dimensions as an adjacent phase change material layer.

It would have been obvious to one of ordinary skill in the art at the time of invention was made, to

Although the reference of Chen teaches intermediate conductive layers has a greater height and greater thickness than the height and thicknesses of each of the phase change material layers, it would have been obvious to one of ordinary skill in the art at the time of invention was made, that the intermediate conductive layers have the same width (see fig. 3) and depth (layers interlaced with the phase change material,

which is written on having the same depth), therefor having intermediate conductive

layers having same dimensions with the phase change material layers.

As for claim 11, Chen discloses the phase change material layers are made of

Ge.sub.2Sb.sub.2Te.sub.5 (col.4, l.52).

As for claim 12, Chen discloses the plurality of conductive layers are made of W,

TiW, etc. (col.4, l.44).

As for claim 13, Chen demonstrates the number of phase change material layers

corresponds to the number of possible bit values storable (col.4, l. 36-38).

As for claim 22, Chen expresses memory technologies can be read only, write

once only, or repeatedly read/write which represents a programming circuit that writes

data to the array of multi-bit phase change memory cells; and a sensing circuit that

reads out data from the array of multi-bit phase change memory cells. All other

limitations of claim 22 are discussed above.

As for claim 23, see discussion to claim 11.

With respect to newly added claims 26-29, all limitations have been previously

presented, and therefor are discussed in the rejection above.

Claim Rejections - 35 USC § 103

Claims 9, and 10 are rejected under 35 U.S.C. 103(a) as being unpatentable

over Chen and Lowrey, in view of Klersy et al. of USPN 5,536,947.

Chen fails to demonstrate the plurality of phase change material layers are of similar resistivity (as in applicants' claim 3), and are made of the same or different material (as in claims 9 and 10).

Klersy et al. teaches compositional modification of phase change materials, including use of any means to modifying the compositions, such as modifying: the volume to yield stable values of resistance, which points to the plurality of phase change material layers having different dimensions (as in applicants' claim 6); and the phase change material layers made of the same or different material, as in claims 9 and 10 (col.14, l.3-54).

Claim Rejections - 35 USC § 103

Claim 8 is rejected under 35 U.S.C. 103(a) as being unpatentable over Chen and Lowrey, as discussed above, in view of Ovshinsky et al. of US 2004/0178401.

Chen fails to teach, the limitation to structure as recited in claim 8.

Ovshinsky illustrates all the limitations of claim 8 in figure 3, and explained in Example 1: a dielectric layer (60) formed between the first outer electrode (90) and the second outer electrode (30) and along sides of at least one other conductive layer (70) and a phase change material layer (80) disposed directly adjacent to the at least one other conductive layer (110).

It would have been obvious to one of ordinary skill in the art at the time of invention was made, to modify the invention of multi-bit phase changing memory device, of Chen, to include the structure of forming said device, as Ovshinsky, because

Ovshinsky demonstrates a specific structure exhibits the ability to modulate the threshold voltage between two electrodes of a multi-terminal device by applying a control voltage to a control terminal. This modulation effect represents improved functionality because the structure includes multi-terminal devices, a process improvement to the standard two-terminal devices.

Response to Arguments

Applicants assert, on page 8, that the reference of Klersy is not properly combined with Chen because it does not teach or suggest a muti-bit phase change memory cell (claim 1) or a multi-bit phase change memory (claim 22) wherein each of the phase change material layers have the same resistivity. Klersy teaches a multi-bit single cell memory (i.e. multi-bit memory cell) (see title) and a detailed description of how they function by phase changing (see background and col. 10, lines 15-25), including how a single cell can have multiple bits (see col. 1, line 42 and col.23, line 43), and the switching (i.e. the changing) of the phase material from the amorphous to the crystalline state, which is written on wherein each of the phase change material layers have the same resistivity (see col. 4, lines 41-53).

As to applicants assertion, on pages 8-9, even if the multiple layers of the volume of memory material in Klersy indeed formed of the same alloy, this fact alone may not be dispostive of whether these layers will have-the same resistivity, please see examiners annotation on Chen's teaching above, to provides specific details how the change of phase as in amorphous to the crystalline state or visa versa is written on

each of the phase change material layers have the same resistivity, also see response in the paragraph above which points to Klersy's teaching. It would have been very obvious to one of ordinary skill in the art at the time of invention was made, that a change to the states of the phase change material, as in Kersey or Chen, would indicated the materials having the same resistivity, as applicant's claimed limitation, because it is well known that memory devices are programmed between a generally amorphous state that exhibits a relatively high resistivity, and a generally crystalline state that exhibits a relatively low resistivity and that there are frequent times when the bits of the same cell are in the same state, having the same resistivity either programmed all "1" or all "0".

As to applicants remark, on page 10, that the reference of Chen intermediate conductive layers has a greater height and greater thickness than the height and thicknesses of each of the phase change material layers, examiner agree. However, the reference of Chen clearly illustrates the intermediate conductive layers have the same width (see fig. 3) and teaches that the layers are interlaced with the phase change material, which is written on having the same depth, therefor the intermediate conductive layers have same dimensions with the phase change material layers.

Conclusion

THIS ACTION IS MADE FINAL. Applicant is reminded of the extension of time policy as set forth in 37 CFR 1.136(a).

A shortened statutory period for reply to this final action is set to expire THREE

MONTHS from the mailing date of this action. In the event a first reply is filed within

TWO MONTHS of the mailing date of this final action and the advisory action is not

mailed until after the end of the THREE-MONTH shortened statutory period, then the

shortened statutory period will expire on the date the advisory action is mailed, and any

extension fee pursuant to 37 CFR 1.136(a) will be calculated from the mailing date of

the advisory action. In no event, however, will the statutory period for reply expire later

than SIX MONTHS from the mailing date of this final action.

Any inquiry concerning this communication or earlier communications from the

examiner should be directed to Patricia A. George whose telephone number is

(571)272-5955. The examiner can normally be reached on weekdays between 7:00am

and 4:30pm.

If attempts to reach the examiner by telephone are unsuccessful, the examiner's

supervisor, Nadine Norton can be reached on (571)272-1465. The fax phone number

for the organization where this application or proceeding is assigned is 571-273-8300.
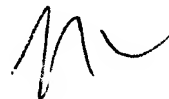
Information regarding the status of an application may be obtained from the

Patent Application Information Retrieval (PAIR) system. Status information for

published applications may be obtained from either Private PAIR or Public PAIR.

Status information for unpublished applications is available through Private PAIR only.

For more information about the PAIR system, see http://pair-direct.uspto.gov. Should

you have questions on access to the Private PAIR system, contact the Electronic

Business Center (EBC) at 866-217-9197 (toll-free). If you would like assistance from a

USPTO Customer Service Representative or access to the automated information

system, call 800-786-9199 (IN USA OR CANADA) or 571-272-1000.

Patricia A George
Examiner
Art Unit 1765

PAG
03/07

NADINE G. NORTON
SUPERVISORY PATENT EXAMINER

U.S. PATENT DOCUMENTS

*		Document Number Country Code-Number-Kind Code	Date MM-YYYY	Name	Classification
*	A	US-6,943,365	09-2005	Lowrey et al.	257/3
*	B	US-6,927,410	08-2005	Chen, Bomy	257/2
*	C	US-5,536,947	07-1996	Klersy et al.	257/3
*	D	US-2004/0178401	09-2004	Ovshinsky et al.	257/002
	E	US-			
	F	US-			
	G	US-			
	H	US-			
	I	US-			
	J	US-			
	K	US-			
	L	US-			
	M	US-			

FOREIGN PATENT DOCUMENTS

*		Document Number Country Code-Number-Kind Code	Date MM-YYYY	Country	Name	Classification
	N					
	O					
	P					
	Q					
	R					
	S					
	T					

NON-PATENT DOCUMENTS

*		Include as applicable: Author, Title Date, Publisher, Edition or Volume, Pertinent Pages)
	U	Jpn. J. Appl. Phys. Vol.39 (2000) 745-751;Part 1, No. 2B, 28 February 2000 Investigation of Crystallization Behavior of Sputter-Deposited Nitrogen-Doped Amorphous Ge2Sb2Te5 Thin Films Hun Seo et al
	V	
	W	
	X	

*A copy of this reference is not being furnished with this Office action. (See MPEP § 707.05(a).)
Dates in MM-YYYY format are publication dates. Classifications may be US or foreign.

Investigation of Crystallization Behavior of Sputter-Deposited Nitrogen-Doped Amorphous Ge₂Sb₂Te₅ Thin Films

Hun SEO*, Tae-Hee JEONG, Jeong-Woo PARK, Cheong YEON, Sang-Jun KIM[1] and Sang-Youl KIM[1]

Devices and Materials Laboratory, LG Corporate Institute of Technology, 16 Woomyeon-Dong, Seocho-Gu, Seoul 137-724, Korea
[1]*Department of Molecular Science and Technology, Ajou University, Suwon 442-749, Korea*

The crystallization behavior of nitrogen-doped amorphous $Ge_2Sb_2Te_5$-(N) phase-change thin films was studied by utilizing differential scanning calorimetry, in situ ellipsometry and in situ transmission electron microscopy. The combined analysis of in situ ellipsometry isotherms of amorphous $Ge_2Sb_2Te_5$-(N) films and the Johnson-Mehl-Avrami equation revealed that the crystallization process of amorphous $Ge_2Sb_2Te_5$-(N) films changes depending on the nitrogen content. The crystallization behavior of $Ge_2Sb_2Te_5$ film revealed a two-step process that includes spherical-nucleation and disc-shaped grain growth. In contrast, nitrogen-doping into $Ge_2Sb_2Te_5$ thin films suppresses the second step and the crystallization of $Ge_2Sb_2Te_5$-(N) becomes a one-step process that is the primary nucleation process. The number of nucleation sites during the crystallization of amorphous $Ge_2Sb_2Te_5$-(N) films, increased markedly with the annealing temperature in the spherically shaped nuclei and eventually saturated. The effective crystallinity of $Ge_2Sb_2Te_5$-(N) alloy films decreased with the increase in nitrogen content, mainly due to the grain-size refinement.

KEYWORDS: nitrogen doping, phase change, Ge₂Sb₂Te₅-(N) thin films, *in situ* ellipsometry, Johnson-Mehl-Avrami equation, nucleation process, grain growth, crystallization, grain size refinement

1. Introduction

The key attributes of promising rewritable storage media include high-speed writing and erasing capability, a sufficient number of overwrite cycles, stable recorded marks, a sufficiently high carrier-to-noise ratio, low and stable jitter characteristics, and good recording sensitivity. The study of chalcogenide alloy thin films used as information storage layers in rewritable phase-change optical media has attracted much attention since the discovery of the optical memory effect of chalcogenides in 1971.[1] Recently, the demand for high-speed, high-density optical recording media using a direct overwrite scheme is very high. Among several chalcogenide material candidates for the recording layer, $Ge_2Sb_2Te_5$ alloy film has been widely studied for this purpose as it has a direct overwrite capability within a short period of time. Hence, considerable interest has been focused on the study of the crystallization behavior of $Ge_2Sb_2Te_5$ alloy.[2-4] Meanwhile, the manipulation of the chemical composition in Ge-Sb-Te-based chalcogenide was attempted by doping a small amount of nitrogen into the Ge-Sb-Te phase-change optical recording layer in order to improve the long-term kinetic properties and recording sensitivity of optical disks.[5,6] In this paper, we report the nitrogen-doping effect on the crystallization behavior of amorphous $Ge_2Sb_2Te_5$ film. The $Ge_2Sb_2Te_5$ film shows an abrupt increase in reflectivity which is proportional to the fraction of the crystalline phase and shows the evolution of the crystallite peak in X-ray diffraction spectra (XRD) after annealing in a general rapid thermal processor (RTP).[4] However, the measurement of the kinetics using *ex situ* reflectivity/XRD after RTP annealing is not adequate because of the very short transition time corresponding to the phase transformation from amorphous to crystalline phase. In this work, this measurement was performed through the combined analysis of Δ and Ψ isotherms by *in situ* ellipsometry and hot-stage transmission electron microscopy (hereafter referred to as *in situ* TEM). The obtained results from the present study were correlated with the Johnson-Mehl-Avrami kinetic formula.[7]

2. Experimental

$Ge_2Sb_2Te_5$-(N) films were deposited on the single crystalline silicon substrates with (100) orientation by DC magnetron reactive sputtering from a target with a nominal chemical composition of $Ge_2Sb_2Te_5$. The sputtering power used in this experiment was 100 W, and background pressure and argon gas pressure were less than 1.4×10^{-5} Pa and 0.67 Pa, respectively. The nitrogen contents of $(Ge_2Sb_2Te_5)_{100-x}N_x$ films in the range of 0–12 at.% were obtained by varying the nitrogen gas flow rate in the range of 0–10 sccm, and argon gas flow rate was fixed at 100 sccm. The chemical composition of the film was determined by combined analysis using inductively coupled plasma spectroscopy-atomic emission spectroscopy (ICP-AES), Rutherford backscattering spectroscopy (RBS), electron spectroscopy for chemical analysis (ESCA) and X-ray fluorescence (XRF). The film thickness of the specimens was about 100 nm. Differential scanning calorimetry (DSC) was employed to measure the crystallization temperatures of amorphous films and the differential thermal analyzer (DTA) for the melting point. Reflectivity measurements and X-ray diffraction analysis were carried out to trace the evolution of crystallization after heat treatment of thin films. *In situ* ellipsometry observations were carried out in order to study the real-time crystallization behavior of $Ge_2Sb_2Te_5$-(N) films. Figure 1 shows a schematic diagram of experimental setup of *in situ* ellipsometry installed in a vacuum chamber. The wavelength of He-Ne laser is 633 nm. The specimen was heated using a halogen lamp at a heating rate of 5°C/min to a preset temperature and was kept constant. The reading and autocontrol of temperature was achieved using a temperature controller and a thermocouple (K-type) forming a tight thermal contact with the rear surface of a specimen. The measured ellipsometry results were also compared with *ex situ* spectroscopic ellipsometry measurements (Uvisel, Jobin Yvon).

For independent confirmation, transmission electron mi-
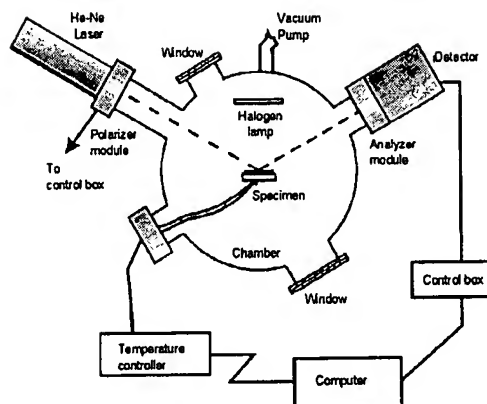
*E-mail address: seoh@lgcit.com

Fig. 1. Schematic diagram of the experimental setup of *in situ* ellipsometry.

Fig. 2. DSC curves for $(Ge_2Sb_2Te_5)_{100-x}N_x$ films at a heating rate of $10°C/min$ where the nitrogen content of the film is (a) 0 at.%, (b) 2.9 at.%, (c) 6.8 at.% and (d) 11.8 at.%, respectively.

croscopy (TEM) thin-foil specimens, with which *in situ* ellipsometry measurements were carried out, were finally examined under a Philips CM20 scanning/TEM operating at 200 keV. In addition, *in situ* TEM studies allowing the direct observation of crystallization were performed using hot-stage TEM (JEOL: JEM-200CX). For this purpose, 25-nm-thick $Ge_2Sb_2Te_5$-(N) films were directly sputter-deposited on the carbon-coated TEM grids. The temperature of the hot stage was monitored by using a Pt-PtRh (13%) thermocouple. The real-time crystallization process of amorphous thin films on the TEM hot stage was imaged at different temperatures, and with different nitrogen contents of the film specimens.

3. Results and Discussion

The chemical composition of the starting material (Ge-Sb-Te thin film without nitrogen-doping) and its melting point are Ge : Sb : Te = 23.0 : 22.7 : 44.3 at.% and 610.8°C, respectively. The chemical composition of the thin film specimen determined using ICP-AES reveals a slightly Ge- and Sb-rich composition from the stoichiometric composition of the $Ge_2Sb_2Te_5$ alloy. The measured nitrogen contents of $(Ge_2Sb_2Te_5)_{100-x}N_x$ films were in the range of 0–12 at.%. Figure 2 shows the exothermic heat flow of the thin film sample during heating. The crystallization temperature corresponds to the peak of the differential signal from DSC. At the heating rate of 10°C/min, the measured crystallization temperatures were in the range of 162–240°C, depending on the nitrogen content. Three different crystallization temperatures at different heating rates (5,10 and 20°C/min) were fitted into the Kissinger plot[8] to calculate the activation energy for crystallization. For a constant heating rate, $\varphi = dT/dt$, the Kissinger equation is

$$\ln(T_x^2/\varphi) = c + (E_a/k_B)\cdot T_p^{-1} \qquad (3.1)$$

where T_x is the crystallization temperature, c a constant, E_a the activation energy for phase transformation, and k_B the Boltzmann constant. A plot of $\ln(T_x^2/\varphi)$ versus $1/T_x$ yields a straight line. The activation energy for the crystallization, E_a, can be calculated from its slope. The crystallization temperature T_x and the activation energy E_a of as-deposited amorphous films increased monotonically with the addition of nitrogen to the $Ge_2Sb_2Te_5$ film (Fig. 3). The increase in T_x and E_a is presumably caused by the nitrogen doping effect

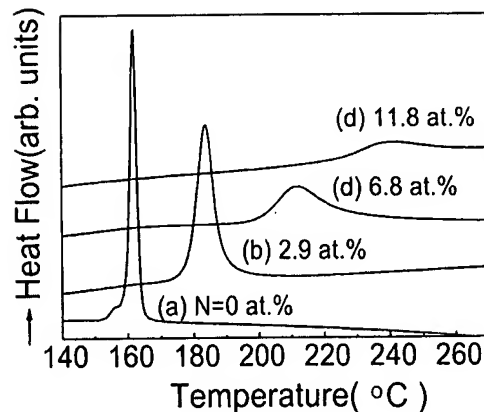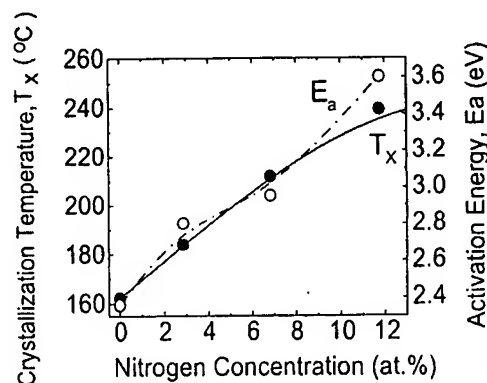Fig. 3. Crystallization temperature and activation energy barrier against crystallization of as-deposited (or amorphous) $Ge_2Sb_2Te_5$-N alloy films as a function of nitrogen content.

which plays the role of an amorphous stabilizer in this alloy system.[6] Referring to the previous work of the authors, $Ge_2Sb_2Te_5$ film shows an abrupt increase in reflectivity and the evolution of the main peak (200) in XRD spectra after 254 s at 140°C.[4] The reflectivity change is proportional to the fraction of the crystalline phase. However, due to the short transition time from the amorphous to crystalline phase, when annealed in a rapid thermal processor (RTP), kinetics measurement using *ex situ* reflectivity/XRD after the RTP method is not adequate. On the contrary, *in situ* ellipsometry appears to be effective for studying the real-time crystallization behavior of amorphous thin films. Figure 4 shows the variation of tan Ψ and cos Δ of undoped $Ge_2Sb_2Te_5$ alloy thin film as a function of annealing time. The ellipsometric constant tan Ψ is the amplitude ratio of the reflection coefficients of p- and s-polarized light, and Δ the phase difference between these two polarized lights, respectively. As can be seen in Fig. 4(a), tan Ψ exhibits a well-known S-shaped transformation curve similar to the reflectivity trend. However, as shown in Fig. 4(b) the change of cos Δ exhibits an additional feature, that is, an abrupt increase during crystallization followed by a gradual decrease immediately after its maximum. The plot of the complex refractive indices, as shown in Fig. 4(c), calculated from the ellipsometric isotherms strongly suggests that
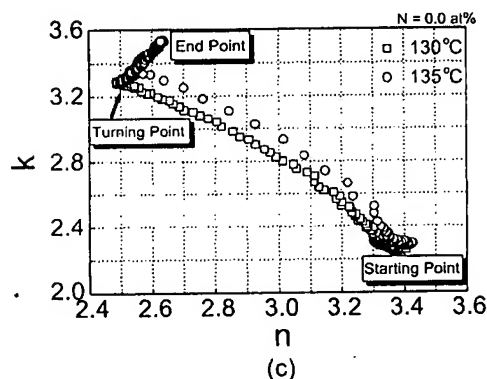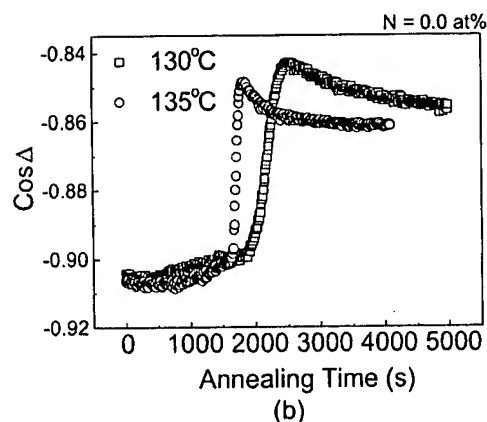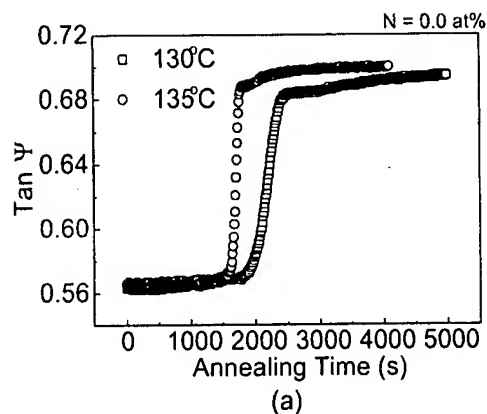
Jpn. J. Appl. Phys. Vol. 39 (2000) Pt. 1, No. 2B

H. SEO et al.   747

(a)

(b)

(c)

Fig. 4. Variation of tan Ψ and cos Δ of undoped Ge₂Sb₂Te₅ alloy film as a function of annealing time and the resulting refractive index change at two selected temperatures of 130°C and 135°C, respectively. Specimens were heated from room temperature at the rate of 5°C/min to the preset temperatures and then maintained at a constant temperature thereafter. (a) tan Ψ vs. annealing time, (b) cos Δ vs. annealing time and (c) trajectory of the complex pseudo-refractive index calculated from Ψ and Δ isotherms.

the crystallization process of Ge₂Sb₂Te₅ film is not simply a one step process but a two-step process. Clearly, amorphous Ge₂Sb₂Te₅ film (start point) is transformed to the crystalline state (end point) via a turning point.

The Johnson-Mehl-Avrami (JMA) equation was also employed for the analysis of the crystallization behavior of the Ge₂Sb₂Te₅-(N) films. Figure 5 shows a schematic representation of the crystallization behavior related to the JMA equation. In the JMA equation, the degree of crystallization V_c is expressed as follows:
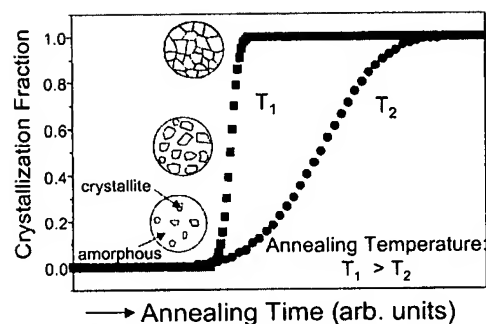

Fig. 5. Calculated variation of crystallization fraction versus annealing time for different transformation temperatures using the Johnson-Mehl-Avrami equation.

Table I. Summary of Avrami exponents and activation energies for the two different crystallizing stages of amorphous Ge₂Sb₂Te₅ phase-change alloy thin film.

Annealing temperature(°C)	1 st stage		2 nd stage	
	n	E_a	n	E_a
130	3.56	2.26	1.15	1.98
135	3.96		1.03	
140	4.50		1.05	
145	5.75		1.25	

$$V_c = 1 - \exp(-Kt^n), \qquad (3.2)$$

$$K = K_0 \exp(-E_a/k_B T), \qquad (3.3)$$

where n is the kinetic exponent and K a rate constant. Provided that there is no change in the nucleation mechanism, n is independent of temperature. K, on the other hand, depends on the nucleation and growth rates and is therefore very sensitive to temperature.[9] From these equations, it can be considered that the transformation rate of the material system with larger n and K is higher than that of smaller systems. At each annealing temperature, the kinetic exponent is evaluated by fitting the corresponding ellipsometry isotherms into the JMA equation. The degree of crystallization can be identified as the volume fraction of the crystalline phase. The fittings are carried out to the first stage between the starting point and the turning point, as well as to the second stage between turning point and the end point. The resulting kinetic exponents and the activation energies for two different stages are listed in Table I. At the first stage, the kinetic exponent n was around 4.4 (3.6–5.8), indicating that nucleation is a dominant stage and the shape of the nuclei is spherical or equiaxial. At the second stage, n was around 1.1 (1.0–1.3); thus, disc-shaped grain growth proceeds. The suggested crystallization process of Ge₂Sb₂Te₅ is that the nucleation occurs in a spherical shape at the initial stage until it becomes saturated and then the disc-shaped grain growth continues in the film. Figure 6 and 7 show the variations of tan Ψ and cos Δ of nitrogen-doped Ge₂Sb₂Te₅ alloy thin films as a function of annealing time. Figure 6 shows the case with 2.9 at.% nitrogen content, and as can be seen in Fig. 6(a), tan Ψ exhibits the general S-shaped transformation curve. In addition, the change of cos Δ in Fig. 6(b) does not exhibit the extraordinary feature appearing in the case of undoped Ge₂Sb₂Te₅ as shown in Fig. 4(b). cos Δ shows an abrupt increase during
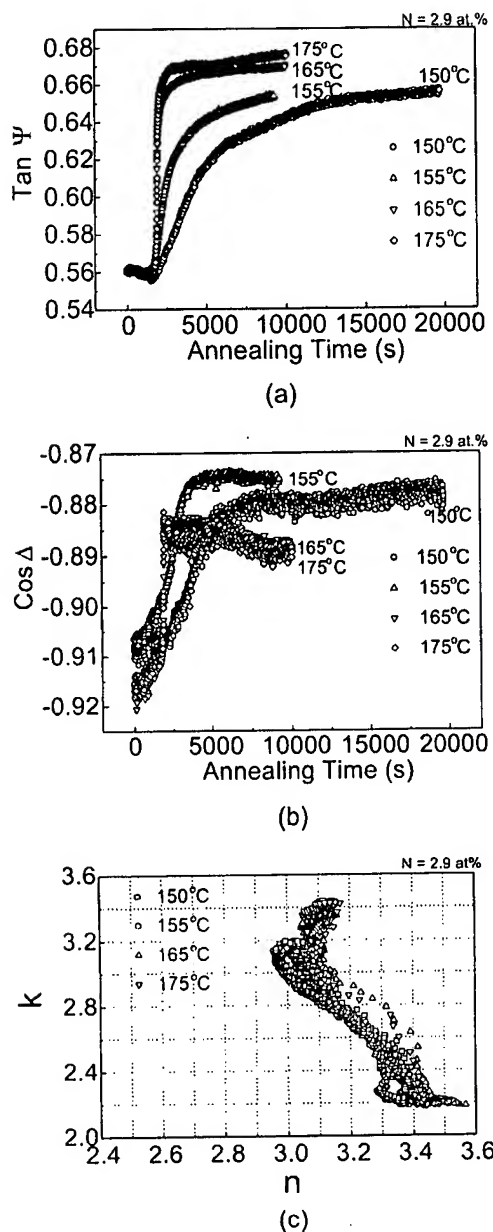
Fig. 6. Variation of tan Ψ and cos Δ as a function of annealing time and the resulting refractive index change of $Ge_2Sb_2Te_5$-N alloy film with 2.9 at.% nitrogen content at four different temperatures. Specimens were heated from room temperature at the rate of 5°C/min to the preset temperatures and then maintained at constant temperature thereafter. (a) tan Ψ vs. annealing time, (b) cos Δ vs. annealing time and (c) trajectory of the complex pseudo-refractive index.

Fig. 7. Variation of tan Ψ and cos Δ as a function of annealing time and the resulting refractive index change of $Ge_2Sb_2Te_5$-N alloy film with 6.8 at.% of the nitrogen content at four different temperatures. Specimens were heated from room temperature at the rate of 5°C/min to the preset temperatures and then maintained at constant temperature thereafter. (a) tan Ψ vs. annealing time, (b) cos Δ vs. annealing time and (c) trajectory of the complex pseudo-refractive index.

crystallization, followed by gradual saturation. The plot of the complex refractive indices does not show a clear turning point (Fig. 6(c)) either. Thus, it can be suggested that the crystallization process of $Ge_2Sb_2Te_5$ film having 2.9 at.% of nitrogen is not a definite two-step process but instead is closer to a one-step process. Figure 7 shows the case with 6.8 at.% nitrogen content, and as can be seen in Figs. 7(a) and 7(b), tan Ψ and cos Δ isotherms show the ordinary transformation curves. The plot of the complex refractive indices, as shown in Fig. 7(c), does not exhibit any turning point at all. The crystallization process of $Ge_2Sb_2Te_5$ film with 6.8 at.% nitro-
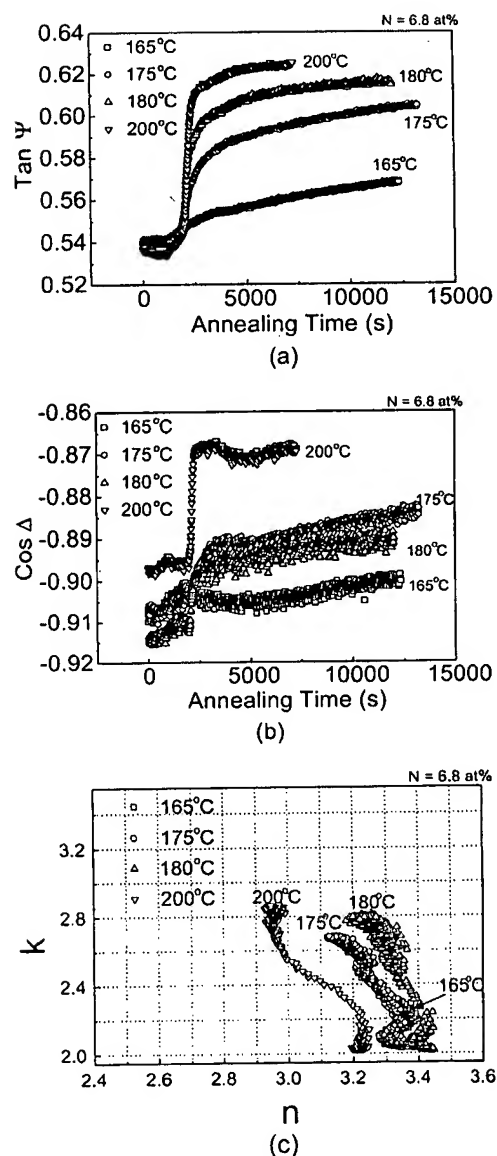
gen is primarily a one-step process. From the observations of the crystallization kinetics using isothermal *in situ* ellipsometry analysis, we can conclude that the maturity of phase transformation during isothermal annealing in the moderate temperature range of 150–200°C becomes insufficient as the nitrogen content is increased. This insufficient phase transformation caused by the nitrogen doping confirms the suggested nitrogen doping effect as an amorphous stabilizer in this alloy.[6] Figure 8 shows the JMA kinetic exponents calculated from the combined analysis of *in situ* ellipsometry isotherms and the JMA equation as a function of annealing temperature, with respect to the three different nitrogen contents. On the basis of this figure, it is proposed that the kinetic exponent *n*
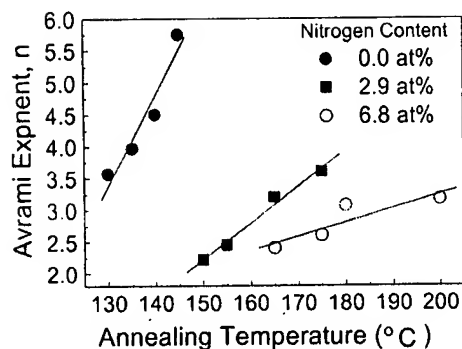
Fig. 8. Effect of nitrogen doping into $Ge_2Sb_2Te_5$ alloy film and of annealing temperature on the Avrami kinetic exponent, n.
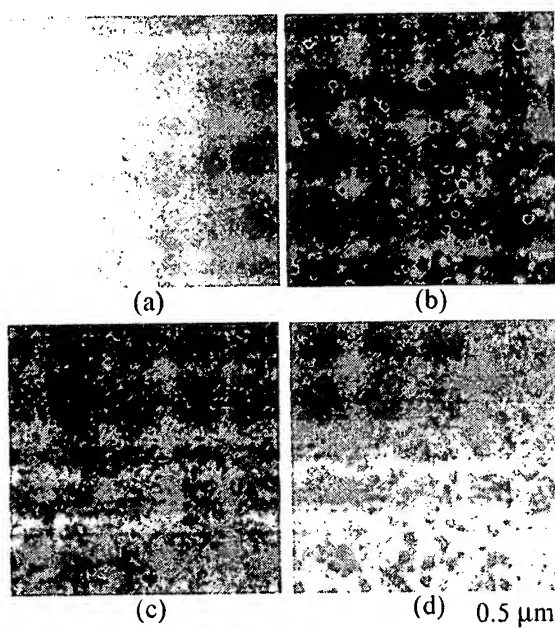

Fig. 10. TEM micrographs showing the initial stage of the crystallization process of amorphous $Ge_2Sb_2Te_5$-N alloy film with 2.9 at.% of nitrogen by in situ TEM with a hot stage at 175°C in the sequence of (a), (b), (c) and (d).

Fig. 9. TEM micrographs showing the initial stage of the crystallization process of undoped amorphous $Ge_2Sb_2Te_5$ thin film by in situ TEM with a hot stage at 140°C in the sequence of (a), (b), (c) and (d).

Fig. 11. TEM micrographs showing the initial stage of the crystallization process of the amorphous $Ge_2Sb_2Te_5$-N alloy film with 6.8 at.% nitrogen by in situ TEM with a hot stage at 205°C in the sequence of (a), (b), (c) and (d).

increases with increasing annealing temperature, that is, empirically n is not a constant but a variable that depends on temperature. In other words, the change of the kinetic exponent is presumed to be caused by the alteration of the nucleation mechanism as a function of the temperature of phase transformation in this Ge-Sb-Te alloy system. In addition, it is noted that n decreases as nitrogen content increases. The combined effect of decreasing n and increasing activation energy with the increase of nitrogen content to the transformation kinetics from amorphous to crystalline is to reduce the nucleation and growth rate, which, in turn, is closely related to the improved stability of the amorphous phase.

In addition to in situ ellipsometric analysis, the crystallization mechanism was independently verified by the combined use of in situ and ex-situ TEM analysis. The in situ TEM images are shown in Figs. 9, 10 and 11 with the sequence of the nitrogen content of 0, 2.9 and 6.8 at.%, respectively. The annealing temperatures of the TEM hot-stage were fixed at
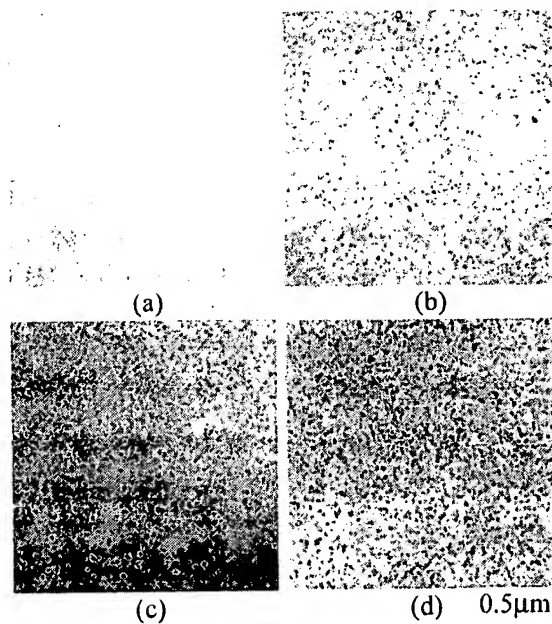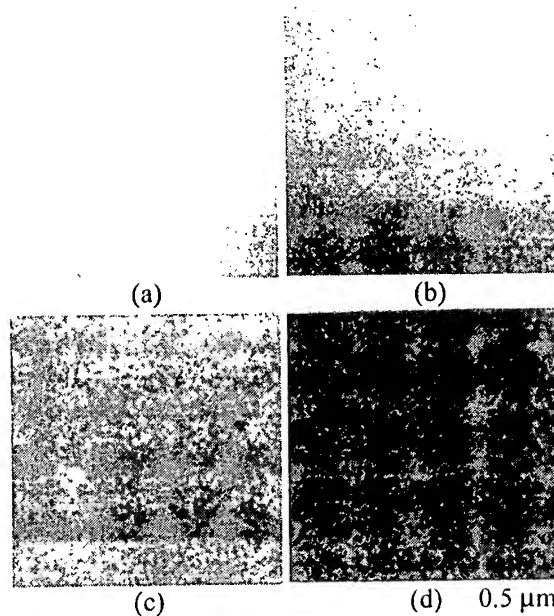
slightly above the highest temperatures of the in situ ellipsometry experiments. In the case of without nitrogen-doping, when the temperature of the hot stage reached 140°C, the crystallization process proceeds in the course of (a)→ (b)→ (c)→ (d), as shown in Fig. 9. TEM images showing the crystallization process in this figure were taken every 2 s. As is
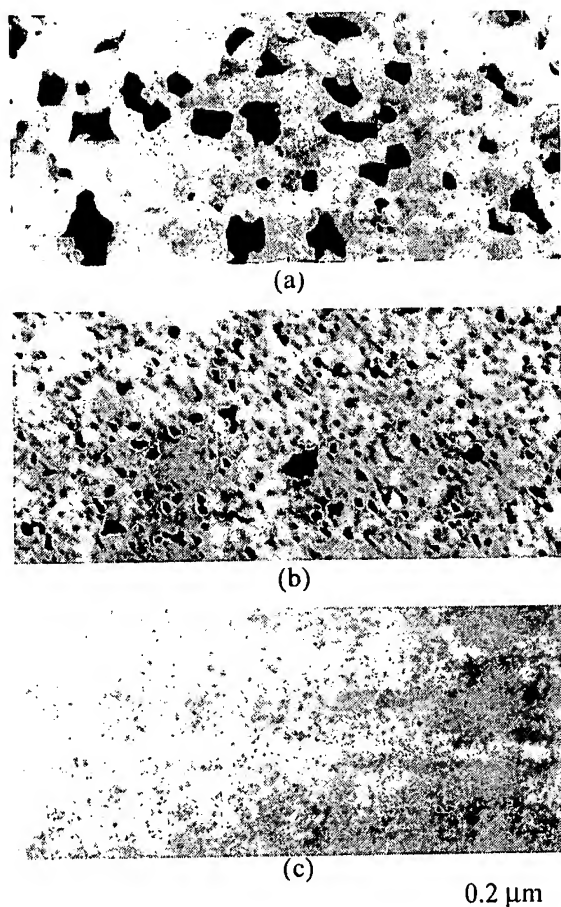
Fig. 12. TEM micrographs after site-saturation during the crystallization process of nitrogen-doped $Ge_2Sb_2Te_5$ alloy film by *in situ* TEM with a hot stage. (a) $N = 0$ at.%, (b) 2.9 at.% and (c) 6.8 at.%.

Fig. 13. Effective crystallinity versus annealing temperature with respect to three different nitrogen contents of $Ge_2Sb_2Te_5$-N alloy films. d_{TEM} in parenthesis is average grain size measured from *in situ* TEM micrographs after site-saturation during annealing.

clearly seen in the figure, the initial progress of crystallization occurs as a spherical or equiaxial shape in the amorphous matrix at the beginning of the nucleation stage. This nucleation reaches site-saturation with equiaxial grains of an average size of ~70 nm in diameter, as shown in Fig. 9(d), and this state is presumed to correspond to the vicinity of the turning point of *in situ* ellipsometric variation in the n vs. k plane, as shown in Fig. 4(c). Following the completion of stage 1, the crystallization further proceeds by the coalescence of the grains and results in a final grain size of up to ~1 μm.[4]

On the contrary, in the case of $Ge_2Sb_2Te_5$-N thin film, the crystallization process could be considered to be a one-step process which is primarily the nucleation process resulting in grain refinement. This is clearly shown in Fig. 10 in the case of 2.9 at.% nitrogen content. The grain size reaches about ~20 nm immediately after the site-saturation, as shown in Fig. 10(d), and the grain size does not increase above ~0.1 μm even after prolonged annealing. Meanwhile, in the case of $Ge_2Sb_2Te_5$-N thin film with 6.9 at.% nitrogen content, the average grain size is ~10 nm at most, as shown in Fig. 11(d). The grain-refinement effect due to nitrogen doping is clearly shown in Fig. 12. Finally, we introduce the concept of effective crystallinity which reflects both the degree of intrinsic crystallinity and the generated defects inside the
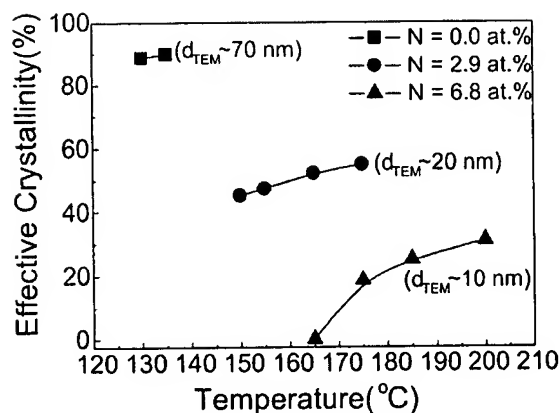
film (i.e., grain boundaries and other defects including strain field, etc.). The single crystalline phase without any generated defects inside the film will have 100% effective crystallinity. The effective crystallinity can be calculated from the model analysis of *ex situ* spectroscopic ellipsometry data after thermal annealing, where the effective volume fraction of the crystalline phase in the film is defined as the effective crystallinity. Figure 13 shows the effective crystallinity of $Ge_2Sb_2Te_5$-(N) alloy thin films after thermal annealing. From this figure, it is evident that there is a strong correlation between the effective crystallinity and the grain size refinement of the $Ge_2Sb_2Te_5$-(N) alloy thin films, that is, the effective crystallinity and grain size decrease in the same manner with increasing nitrogen content.

4. Conclusions

The crystallization behavior of nitrogen-doped amorphous $Ge_2Sb_2Te_5$-(N) phase-change thin films has been investigated. The combined analysis of *in situ* ellipsometry isotherms of amorphous $Ge_2Sb_2Te_5$-(N) thin films and the JMA equation revealed that the crystallization process changes depending on the nitrogen content of $Ge_2Sb_2Te_5$-(N) films. The crystallization behavior of undoped $Ge_2Sb_2Te_5$ thin film was found to be a two-step process consisting of the formation of spherical nuclei and disc-shaped grain growth after prolonged annealing. However, the crystallization behavior of nitrogen-doped $Ge_2Sb_2Te_5$ thin films could be primarily a one-step process of nucleation. The marked increase of the nucleation and growth rate with increasing annealing temperature during the crystallization of amorphous $Ge_2Sb_2Te_5$-(N) thin films is suppressed in proportion to the nitrogen content. This was confirmed by TEM analysis. The effective crystallinity of $Ge_2Sb_2Te_5$-(N) alloy films decreased with the increase of nitrogen content mainly because of the grain-size refinement. The combined effect of the decreasing kinetic exponent and increasing activation energy with the increase of nitrogen content is to reduce the nucleation and growth rate in connection with the improved stability of the amorphous phase of $Ge_2Sb_2Te_5$-(N) alloy films.

1) J. Feinleib, J. de Neufville, S. C. Moss and S. R. Ovshinsky: Appl. Phys. Lett. **18** (1971) 254.
2) J. Gonzalez-Hernandez, B. S. Chao, D. Strand, S. R. Ovshinsky, D. Pawlik and P. Gasiorowski: Appl. Phys. Commun. **11** (1992) 557.
3) N. Yamada, E. Ohno, K. Nishiuchi, N. Akahira and M. Takao: J. Appl. Phys. **69** (1991) 2849.
4) T. H. Jeong, M. R. Kim, H. Seo, S. J. Kim and S. Y. Kim: J. Appl. Phys. **86** (1999) 774.
5) R. Kojima, S. Okabayashi, T. Kashihara, K. Horail, T. Matshunaga, E. Ohno, N. Yamada and T. Ohta: Jpn. J. Appl. Phys. **37** (1998) 2098.
6) M. R. Kim, H. Seo, T. H. Jung, J. W. Park and C. Yeon: Tech. Dig. Optical Data Storage, Aspen Colorado (1998) PD5-2.
7) J. W. Christian: *The Theory of Transformations in Metals and Alloys* (Pergamon Press, New York, 1975) 2nd ed., Chap. 12, p. 526.
8) H. E. Kissinger: Anal. Chem. **29** (1957) 1702.
9) D. A. Porter and K. E. Easterling: *Phase Transformations in Metals and Alloys* (Van Nostrand Reinhold, New York, 1981) Chap. 5, p. 290.